Heliyon 9 (2023) e13865

Contents lists available at ScienceDirect

Heliyon

journal homepage: www.cell.com/heliyon

Research article

Carrier transport and photoconductivity properties of BN_{50}/NiO_{50} nanocomposite films

Manjot Kaur [a,1], Kulwinder Singh [a,b,1], Ram K. Sharma [c], Nandni Sharma [d], Anup Thakur [e], Akshay Kumar [f,*]

[a] University Centre for Research and Development, Chandigarh University, Mohali, 140413, Punjab, India
[b] Department of Chemistry, University Institute of Sciences, Chandigarh University, Mohali, 140413, Punjab, India
[c] Centre for Interdisciplinary Research, University of Petroleum and Energy Studies (UPES), Dehradun, 248007, Uttarakhand, India
[d] Department of Physics, University Institute of Sciences, Chandigarh University, Mohali, 140413, Punjab, India
[e] Advanced Materials Research Lab, Department of Physics, Punjabi University Patiala, 147 002, Punjab, India
[f] Department of Physics, Sardar Patel University, Mandi, Himachal Pradesh, 175001, India

ARTICLE INFO

Keywords:
Nanocomposites
Thin films
Defects
Surface plasmon resonance
Photoconductivity

ABSTRACT

BN_{50}/NiO_{50} and Au-loaded BN_{50}/NiO_{50} nanocomposite films were separately fabricated on the glass substrates for carrier transport and photoconductivity properties. X-ray diffraction pattern of the films show the hexagonal structure of BN and presence of defect states by Nelson Riley factor analysis. Morphological images show spherical shaped particles with highly porous structure. The incorporation of NiO may hindered growth of BN layers and resulted in spherical particles. Temperature-dependent conductivity describes semiconductor transport behaviour for deposited nanocomposite films. Thermal activation conduction with low activation energy (~0.308 eV) may be responsible for the resulting conductivity. Further, the light intensity dependent photoelectrical properties of BN_{50}/NiO_{50} and Au-loaded BN_{50}/NiO_{50} nanocomposites have been explored. The effect of Au nanoparticles loading on enhanced photo-conductivities (~22% increase) than bare nanocomposite film has been elaborated by proposed mechanism. This study provided the insightful information for carrier transport and photoconductivity of BN-based nanocomposites.

1. Introduction

Two dimensional (2D) materials are under tremendous research due to their unique optical, structural and electronic properties [1]. These materials have been explored for several applications such as gas sensors, lithium-ion batteries, photodetectors, transparent and flexible electronics, supercapacitors, catalysis, etc. [2–4]. Graphene is one of the effective 2D material in fundamental as well as applied science [5,6]. Graphene alike boron nitride (BN) has potential to be explored in optoelectronic and sensing applications due to its tunable properties [7,8]. Hexagonal BN (h-BN) is one of the van-der-Waals 2D semiconductor with exceptional properties to be used in diverse filed of applications extending from optoelectronic, sensors to biomedical [9,10].

BN nanostructures possess properties comparable to its carbon counterparts. h-BN own large bandgap energy (~ 4 eV to ~ 6 eV), in

* Corresponding author.
E-mail address: akshaykumar.tiet@gmail.com (A. Kumar).
[1] Equal Contribution.

https://doi.org/10.1016/j.heliyon.2023.e13865
Received 3 November 2022; Received in revised form 9 February 2023; Accepted 14 February 2023
Available online 18 February 2023

part ionic character, honeycomb crystal lattice with sp^2-hybridized atoms. h-BN with different morphologies such as nanoparticles, nanosheets, nanotubes, nanorods, nanoflakes, etc. has been reported [11,12]. For preparation of BN, several methods such as arc discharge, solvothermal method, chemical vapor deposition, chemical exfoliation, ball milling, laser ablation, etc. has been used [13, 14]. The properties of h-BN can be further improved by hybridization with other semiconductor materials. Various superlattice materials and binary compounds have been studied for structural, electronic and optical properties [15–19]. Some theoretical as well as experimental studies show superior properties by doping, element incorporation, composite formation or functionalization of BN nanostructures [20–23]. Hybrid systems or nanocomposites may help to form multi-functional devices owing to improved properties than the separate compounds.

On the other hand, nickel oxide (NiO) is a p-type semiconducting metal oxide with energy bandgap in the range of 3.6–4.0 eV, high chemical stability, exceptional electrical and optical properties. NiO has been studied for solar cells, optoelectronic and sensing applications [24–27]. In NiO (partial covalent solid), Ni and O attain positive and negative charges, respectively. It interacts with oppositely charged N and B of BN to form a composite. These interactions can lead to crystal structure distortion or incorporation of defect states in this BN-based composite which may help in property enhancement [28]. NiO nanocomposite with BN can tune band gap of BN to work in visible region. Also, its p-type nature makes it suitable to be explored for electrical and opto-electrical properties.

In present work, BN_{50}/NiO_{50} nanocomposite has been synthesized by modified chemical method. Then BN_{50}/NiO_{50} nanocomposite films have been deposited by drop casting method on glass substrates. Electrical properties with temperature variation have been explored for carrier transport mechanism. Further, photo-electrical measurements were carried from dark to 1750 lux light intensity. Effect of gold (Au) nanoparticles loading on photoconductivity has also been elaborated with a mechanism.

2. Experimental details

For the preparation of BN_{50}/NiO_{50} nanocomposite structures, modified chemical method was used. More details can be found in previous report [29]. For briefing, the process involves the dissolution of nickel nitrate hexahydrate in DI water and methanol containing solution followed by stirring for 2 h. Appropriate quantities of solvothermal prepared BN nanostructures have been added to the solution followed by stirring for 2 h. Ammonia solution was used for precipitation of the above solution followed by stirring for another 2 h. After drying the obtained product, the product is subjected at 550 °C for annealing purpose for 4 h. The final material is

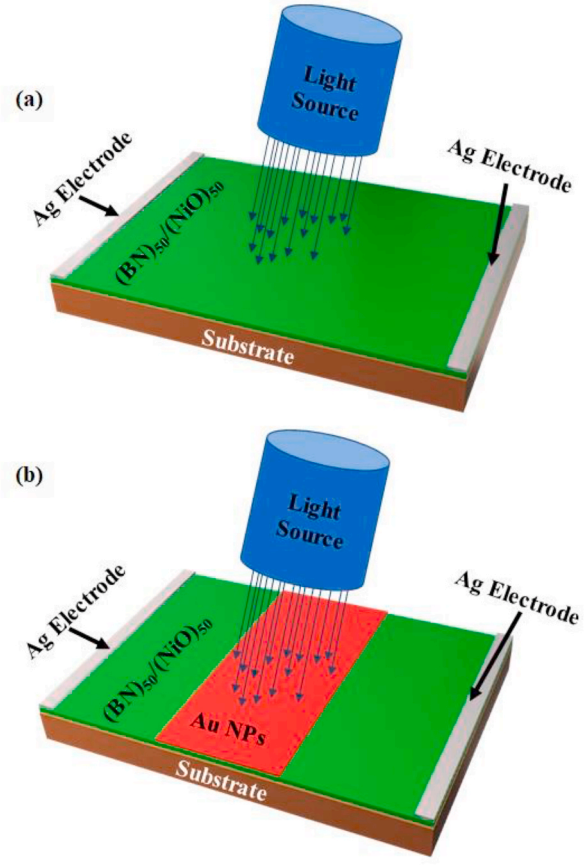

Fig. 1. Schematic of device structure (a) Bare BN_{50}/NiO_{50}, and (b) Au nanoparticles loaded-BN_{50}/NiO_{50} film respectively.

characterized and used for deposition of film on glass substrate. For film deposition, the 5 mg powder of synthesized sample was dissolved in 1 ml water followed by ultrasonication for 1 h. Approximately, 100 μl sample solution was drop-casted on the glass substrate with the help of micro-pipette prior to drying for 1 h in vacuum oven at 70 °C. The final deposited samples are characterized for structural, morphological and electrical properties. Structural properties of the deposited film samples were investigated with the help of Diffractometer (Rigaku). To obtained the XRD patterns, 1.5406 Å wavelength radiations (Cu K_α) were utilized. Sigma Carl Ziess FESEM was employed for checking the morphological properties and cross-sections of the deposited samples.

To measure the electrical properties of the deposited samples, electrodes have been made on the deposited film with the help of Ag conducting paste. Current variations with respect to the variation of temperature have been studied in detail. Sourcemeter (Keithley-2450) computer interfaced MS-TECH probe station was employed to measure the current-voltage characteristics in the voltage sweep mode ranging from −10 V to +10 V, of the deposited film sample. Furthermore, the effect of Au nanoparticles loading on electrical properties of the deposited film sample was also investigated under dark as well as exposure to different light intensities. Fig. 1(a and b) shows the schematic of used device structure of bare and Au nanoparticles loaded BN_{50}/NiO_{50} to investigate electrical properties under exposure to light intensities.

3. Results and discussion

XRD pattern, Raman analysis, UV–visible spectroscopy and bandgap analysis of BN_{50}/NiO_{50} nanocomposite powder sample is reported in our earlier work [29]. XRD pattern of deposited BN_{50}/NiO_{50} nanocomposite film is shown in Fig. 2(a) which is well indexed with BN (ICDD #01-073-2095) and NiO (ICDD #44-1159), respectively. Hexagonal crystal structure of BN has been observed [30]. NiO accumulation in the BN crystal structure generates defect states which leads to the broadening of diffraction peaks. For reference, XRD pattern of BN film is provided in Fig. S1. Fig. 2(b) shows the Nelson-Riley Factor (NRF) plot for deposited nanocomposite films. In comparison to pure BN film, nanocomposite film demonstrates large scatteredness which can be interpreted as presence of defect states in nanocomposite films. The role of these defect states has been discussed in electrical and photoconductivity studies. FESEM image of deposited BN_{50}/NiO_{50} nanocomposite is shown in Fig. 3(a). Spherical morphology with porous structure has been observed due to the incorporation of NiO. The cross-section analysis show ~15.26 μm thickness of deposited thin films (Fig. 3(b)). FESEM image of pure BN film is shown in Fig. S2. The synthesized pure BN has a layered structure as reported in our earlier work, but the accumulation of NiO in

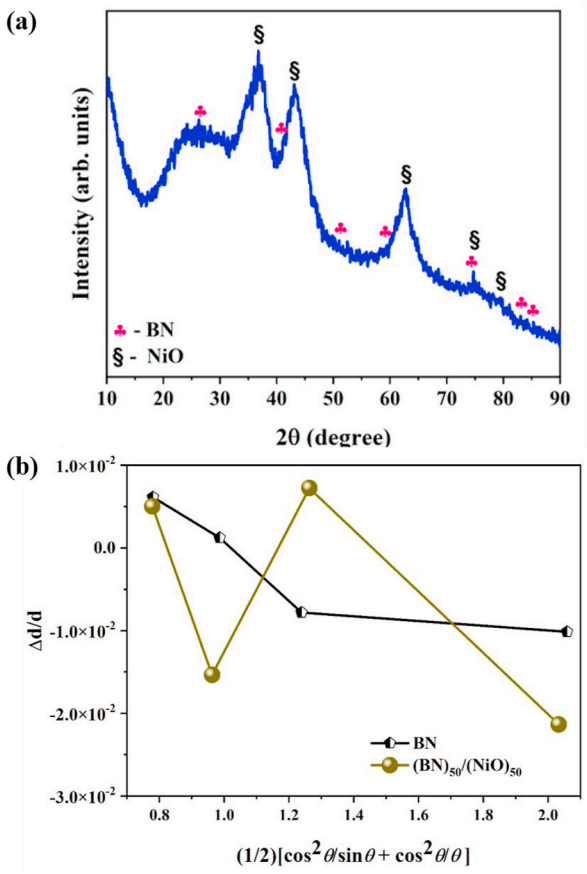

Fig. 2. (a) XRD pattern of BN_{50}/NiO_{50} nanocomposite film; (b) NRF plot for BN and BN_{50}/NiO_{50} nanocomposite film.

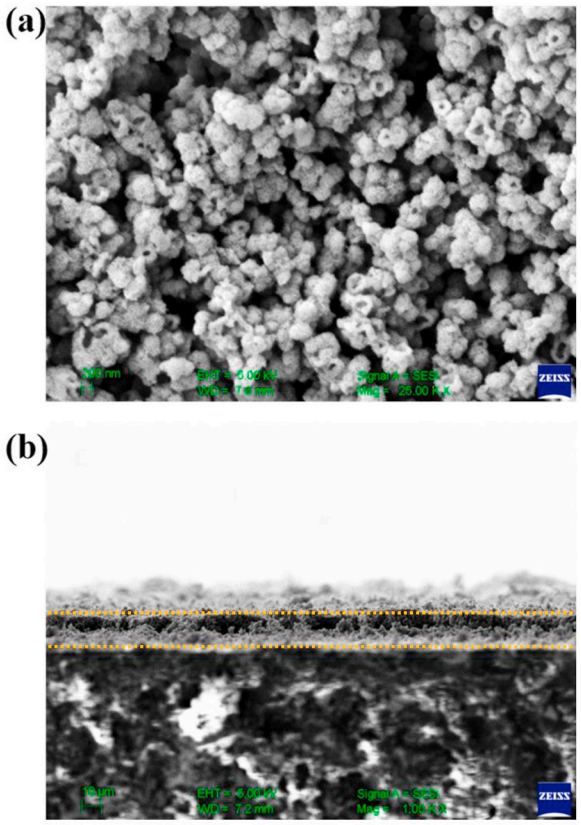

Fig. 3. (a) FESEM image and; (b) Cross-sectional image of BN_{50}/NiO_{50} nanocomposite film.

the BN matrix may have caught up the growth of BN layers of BN which resulted in spherical particles.

Fig. 4(a) shows the temperature-dependent current plot as a function of the voltage. It shows the linear current variation with applied voltage across contacts confirming ohmic nature. The increase in electrical conductivity (σ) of BN_{50}/NiO_{50} nanocomposite film has been observed with the rise in temperature. To realize the carrier transport process with temperature, Fig. 4(b) gives the BN_{50}/NiO_{50} nanocomposite film plot fitted by the Arrhenius equation. In semiconductors, the high temperature conduction process generally hails from the electrons jumping from valence band to acceptor levels or from donor levels to conduction band.

For thermal activated conduction, conductivity (σ) versus temperature (T) relation can be expressed as [31]:

$$\sigma = \sigma_o \, exp\left(-\frac{\Delta E}{kT}\right) \tag{1}$$

where σ_o, k, T and ΔE are pre-exponential factor, Boltzmann's constant, temperature, activation energy, respectively. As shown in Fig. 4(b), experimental data of BN_{50}/NiO_{50} nanocomposite films can be fitted well by Eq. (1) in the temperature range of 25–175 °C. The activation energy of BN_{50}/NiO_{50} nanocomposite films obtained is ~0.30 eV.

The activation energy of BN_{50}/NiO_{50} nanocomposite film is lower as compared to pure BN and NiO [28]. Presence of defects states as confirmed from NRF analysis may have contributed to lower activation energy. The lower value of activation energy results in generation of more charge carriers in a semiconductor. But conductivity in deposited film is slightly less than pure BN and NiO [28] which may have resulted from higher thickness of deposited film.

Fig. 5(a) demonstrated the current variation of BN_{50}/NiO_{50} nanocomposite film corresponding to applied voltages at different light intensities. The light intensities were varied ranging from dark to 1750 lux. As shown in Fig. 1(b), Au-loaded BN_{50}/NiO_{50} nanocomposite film has also been fabricated to observed the effect of gold nanoparticle loading on photoconductivity. Similar current measurements like bare nanocomposite films have been examined for Au nanoparticles loaded films with light intensity variation. Fig. 5(b) shows the photoconductivity studies of Au-loaded BN_{50}/NiO_{50} nanocomposite film. Au nanoparticle loaded BN_{50}/NiO_{50} nanocomposite film shows ~22% increase in photoconductivity than bare BN_{50}/NiO_{50} at various light intensities. Further illumination of photoconductivity dependency of bare deposited and Au-loaded films on light intensities (ln σ_{ph} vs ln F) is shown in Fig. 6. It is observed that photoconductivity of films increased with light intensity increase.

Photoconductivity of Au-loaded BN_{50}/NiO_{50} nanocomposite has been explained by proposing hot-electron based model. When light incidents on metal-semiconductor interface, it leads to hot electron generation. These hot-electrons can boost surface activity [32,

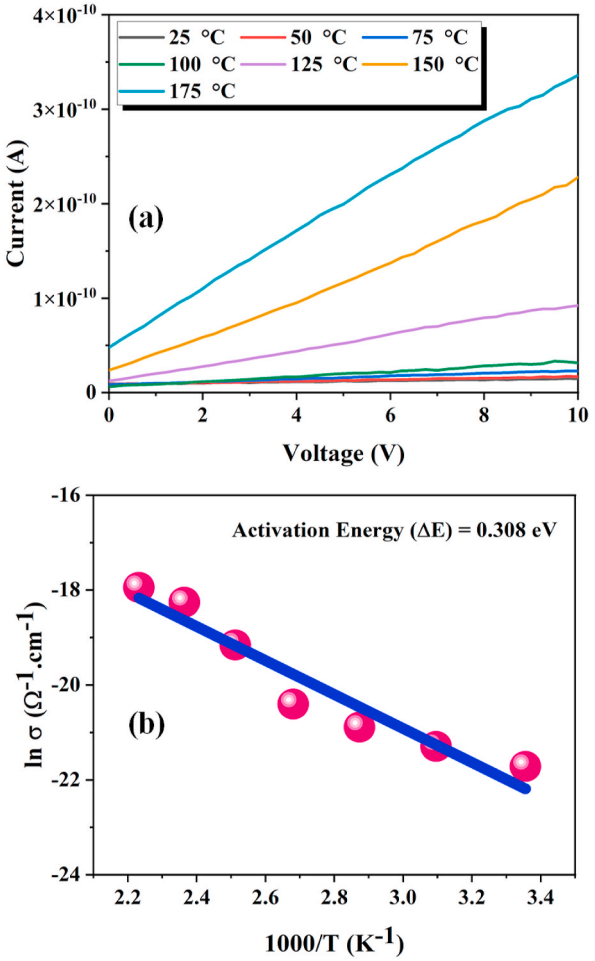

Fig. 4. (a) Voltage vs Current graphs of BN_{50}/NiO_{50} at different temperatures; (b) Temperature vs conductivity plot for BN_{50}/NiO_{50} nanocomposite film.

33]. As shown in Fig. 7(a and b), the light interaction with metal surface may result in localized surface plasmon resonance (LSPR) or light scattering by random surface plasmon polaritons or damping depending upon the incident light [34,35]. These LSPR or surface plasmon polaritons may excite the free electrons in NiO surface which then transfers to BN conduction band (CB) by non-radiative processes. The scattered energy leads to enhanced charge carrier separation. Free electrons oscillate with a resonant frequency redistributing the electron charge densities which leads to LSPR. The hot electron transfer from NiO to BN-NiO interface may happens by ballistic transport [36]. As Fermi level energy of NiO is between the CB and valence band gap of BN, free electrons get moved from NiO to boron nitride CB via interface. Also, the presence of defect states in BN_{50}/NiO_{50} nanocomposite film results in improved electrical conductivity owing to plasmon resonance energy transfer effect (PRET) [33]. Therefore, in case of Au-loaded BN_{50}/NiO_{50} nanocomposite film enhanced photoconductivity may result from – PRET and transfer of more hot electrons generated at NiO surface to BN. Thus, BN_{50}/NiO_{50} nanocomposite film can be further explored for photodetection applications.

4. Conclusions

BN_{50}/NiO_{50} nanocomposite film deposited on glass substrate has been explored for carrier transport process and photoconductivity mechanism. Structural analysis confirms deposited nanocomposite film possess defect states which may play an important role in electrical and photodetection properties. Temperature-dependent electrical studies show increase in conductivity. The lower activation energy in thermally conduction mechanism of nanocomposite film than bare BN may be due to the presence of defect states which enables enhanced surface charge transport. Further light intensity dependent photoconductivity properties of simple and Au-nanoparticles loaded BN_{50}/NiO_{50} nanocomposite films show higher conductivity in the latter at different light intensities. With incident light interaction with Au nanoparticles, hot-electrons generated through LSPR and surface plasmon polariton may be responsible for this. The model has been proposed to explained the enhancement of photoconductivity. The results suggests that BN_{50}/NiO_{50} nanocomposite films can be further explored with concentration variation of metal particles, functionalization, film thickness

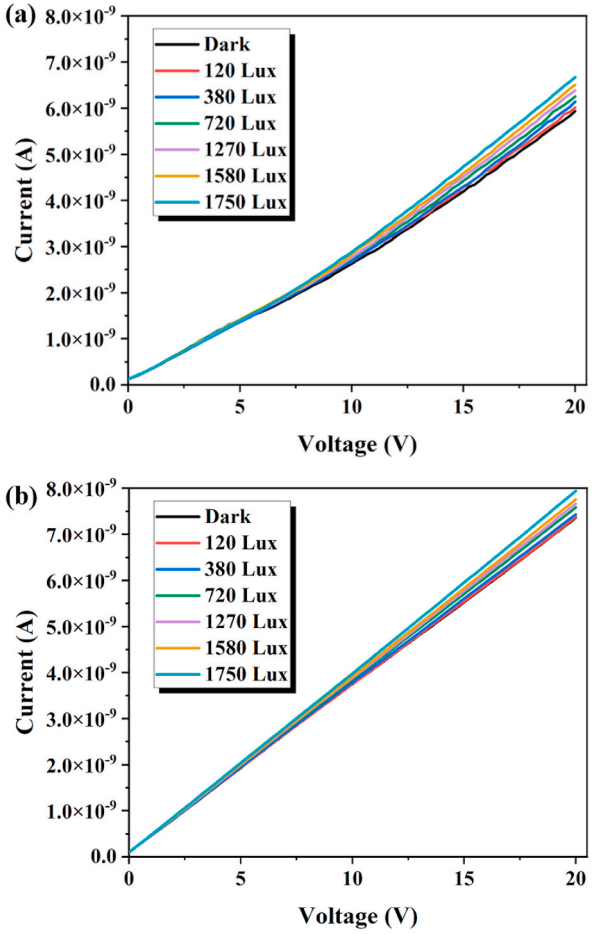

Fig. 5. Voltage vs Current graphs of (a) bare BN_{50}/NiO_{50}; (b) Au-loaded BN_{50}/NiO_{50} nanocomposite films at different light intensities.

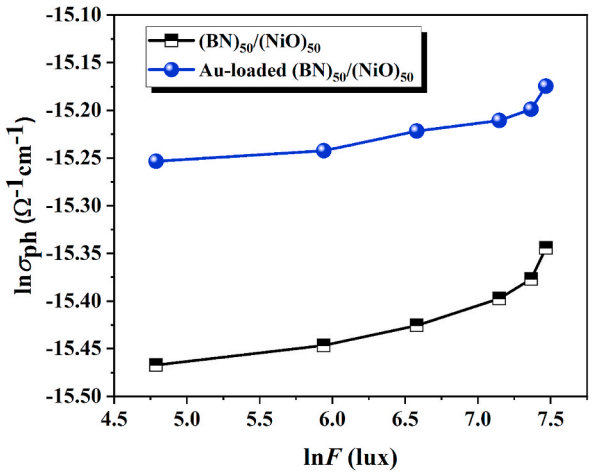

Fig. 6. Light intensity vs conductivity plot for bare and Au-loaded BN_{50}/NiO_{50} nanocomposite films.

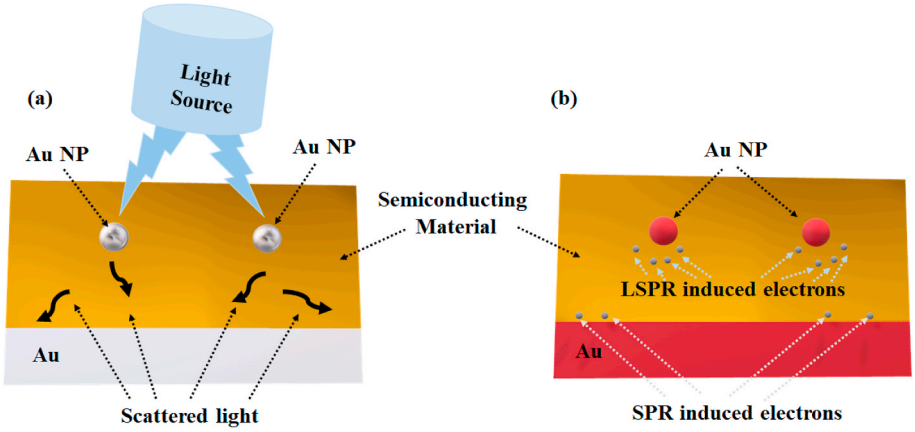

Fig. 7. Mechanism for conductivity enhancement of Au-loaded BN_{50}/NiO_{50} with light exposure: (a) Interaction of incident light with Au nanoparticles; (b) Hot-electron generation.

variation for carrier transport and photodetection applications.

Author contribution statement

Manjot Kaur: Conceived and designed the experiments; Performed the experiments; Analyzed and interpreted the data; Wrote the paper.

Kulwinder Singh, Akshay Kumar: Conceived and designed the experiments; Analyzed and interpreted the data; Contributed reagents, materials, analysis tools or data; Wrote the paper.

Ram K Sharma, Nandni Sharma, Anup Thakur: Analyzed and interpreted the data.

Funding statement

Manjot Kaur was supported by Human Resource Development Group, Council of Scientific and Industrial Research, India [09/1198 (0004)/2020-EMR-I].

Data availability statement

Data will be made available on request.

Declaration of interest's statement

The authors declare that they have no known competing financial interests or personal relationships that could have appeared to influence the work reported in this paper.

Appendix A. Supplementary data

Supplementary data to this article can be found online at https://doi.org/10.1016/j.heliyon.2023.e13865.

References

[1] F.R. Fan, R. Wang, H. Zhang, W. Wu, Emerging beyond-graphene elemental 2D materials for energy and catalysis applications, Chem. Soc. Rev. 50 (19) (2021) 10983–11031, https://doi.org/10.1039/C9CS00821G.

[2] Q. Ma, G. Ren, K. Xu, J.Z. Ou, Tunable optical properties of 2D materials and their applications, Adv. Opt. Mater. 9 (2) (2021), 2001313, https://doi.org/10.1002/adom.202001313.

[3] X. Ling, W. Fang, Y.H. Lee, P.T. Araujo, X. Zhang, J.F. Rodriguez-Nieva, Y. Lin, J. Zhang, J. Kong, M.S. Dresselhaus, Raman enhancement effect on two-dimensional layered materials: graphene, h-BN and MoS_2, Nano Lett. 14 (6) (2014) 3033–3040, https://doi.org/10.1021/nl404610c.

[4] Q. Qiu, Z. Huang, Photodetectors of 2D materials from ultraviolet to terahertz waves, Adv. Mater. 33 (15) (2021), 2008126, https://doi.org/10.1002/adma.202008126.

[5] R. Saito, M. Mizuno, M.S. Dresselhaus, Ballistic and diffusive thermal conductivity of graphene, Phys. Rev. Appl. 9 (2) (2018), 024017, https://doi.org/10.1103/PhysRevApplied.9.024017.

[6] M.S. Dresselhaus, Graphene: a journey through carbon nanoscience, MRS Bull. 37 (2012) 1319–1320, https://doi.org/10.1557/mrs.2012.301.

[7] K.K. Kim, A. Hsu, X. Jia, S.M. Kim, Y. Shi, M. Dresselhaus, T. Palacios, J. Kong, Synthesis and characterization of hexagonal boron nitride film as a dielectric layer for graphene devices, ACS Nano 6 (10) (2012) 8583–8590, https://doi.org/10.1021/nn301675f.

[8] S.M. Kim, A. Hsu, M.H. Park, S.H. Chae, S.J. Yun, J.S. Lee, D.H. Cho, W. Fang, C. Lee, T. Palacios, M.S. Dresselhaus, K.K. Kim, Y.H. Lee, J. Kong, Synthesis of large-area multilayer hexagonal boron nitride for high material performance, Nat. Commun. 6 (2015) 8662, https://doi.org/10.1038/ncomms9662.

[9] A. Hayat, M. Sohail, M.S. Hamdy, T.A. Taha, H.S. AlSalem, A.M. Alenad, M.A. Amin, R. Shah, A. Palamanit, J. Khan, W.I. Nawawi, S.K.B. Mane, Fabrication, characteristics, and applications of boron nitride and their composite nanomaterials, Surface. Interfac. 29 (April 2022) (2022), 101725, https://doi.org/10.1016/j.surfin.2022.101725.

[10] J. Wang, L. Zhang, L. Wang, W. Lei, Z.-S. Wu, Two-dimensional boron nitride for electronics and energy applications, Energy Environ. Mater. 5 (1) (2022) 10–44, https://doi.org/10.1002/eem2.12159.

[11] P. Singla, N. Goel, S. Singhal, Boron nitride nanomaterials with different morphologies: synthesis, characterization and efficient application in dye adsorption, Ceram. Int. 41 (9) (2015) 10565–10577, https://doi.org/10.1016/j.ceramint.2015.04.151.

[12] Z. Zhang, Y. Liu, Y. Yang, B.I. Yakobson, Growth mechanism and morphology of hexagonal boron nitride, Nano Lett. 16 (2) (2016) 1398–1403, https://doi.org/10.1021/acs.nanolett.5b04874.

[13] X.F. Jiang, Q. Weng, X.B. Wang, X. Li, J. Zhang, D. Golberg, Y. Bando, Recent progress on fabrications and applications of boron nitride nanomaterials: a review, J. Mater. Sci. Technol. 31 (6) (2015) 589–598, https://doi.org/10.1016/j.jmst.2014.12.008.

[14] K. Zhang, Y. Feng, F. Wang, Z. Yang, J. Wang, Two-dimensional hexagonal boron nitride (2D-hBN): synthesis, properties and applications, J. Mater. Chem. C 5 (46) (2017) 11992–12022, https://doi.org/10.1039/C7TC04300G.

[15] L. Bahmad, R. Masrour, E.K. Hlil, M. Hamedoun, A. Benyoussef, Couplings and interface effects on magnetic and electronic properties in binary Ni/Cu superlattices, Superlattice. Microst. 63 (2013) 168–181, https://doi.org/10.1016/j.spmi.2013.09.004.

[16] R. Masrour, A. Jabar, Effect of surface and bulk exchange interactions on superlattice materials with a mixed spins: a Monte Carlo study, Solid State Commun. 291 (2019) 15–20, https://doi.org/10.1016/j.ssc.2019.01.004.

[17] S.A. De la Torre Pari, J.C.R. Aquino, A.F. Carlos-Chilo, J.A. Guerra, J.A.H. Coaquira, D.G. Pacheco-Salazar, J.F. Felix, J.L. Solis, F.F.H. Aragón, Enhancing the photoconductivity and gas sensing performance of TiO_2/SnO_2 heterostructures tuned by the thickness of the SnO_2 upper layer, Appl. Surf. Sci. 613 (2023), 156028, https://doi.org/10.1016/j.apsusc.2022.156028.

[18] H. Shu, M. Zhao, M. Sun, Theoretical study of GaN/BP van der Waals nanocomposites with strain-enhanced electronic and optical properties for optoelectronic applications, ACS Appl. Nano Mater. 2 (10) (2019) 6482–6491, https://doi.org/10.1021/acsanm.9b01422.

[19] R. Masrour, A. Jabar, E.K. Hlil, Electronic, magnetic properties and phase diagrams of system with Fe_4N compound: an ab initio calculations and Monte Carlo study, J. Magn. Magn Mater. 453 (2018) 220–225, https://doi.org/10.1016/j.jmmm.2018.01.038.

[20] S.A. Han, K.H. Lee, T.-H. Kim, W. Seung, S.K. Lee, S. Choi, B. Kumar, R. Bhatia, H.-J. Shin, W.-J. Lee, S.M. Kim, H.S. Kim, J.-Y. Choi, S.-W. Kim, Hexagonal boron nitride assisted growth of stoichiometric Al_2O_3 dielectric on graphene for triboelectric nanogenerators, Nano Energy 12 (2015) 556–566, https://doi.org/10.1016/j.nanoen.2015.01.030.

[21] L.-Y. Feng, Y.-J. Liu, J.-X. Zhao, Iron-embedded boron nitride nanosheet as a promising electrocatalyst for the oxygen reduction reaction (ORR): a density functional theory (DFT) study, J. Power Sources 287 (2015) 431–438, https://doi.org/10.1016/j.jpowsour.2015.04.094.

[22] S. Dai, Q. Ma, M.K. Liu, T. Andersen, Z. Fei, M.D. Goldflam, M. Wagner, K. Watanabe, T. Taniguchi, M. Thiemens, F. Keilmann, G.C.A.M. Janssen, S.-E. Zhu, P. J. Herrero, M.M. Fogler, D.N. Basov, Graphene on hexagonal boron nitride as a tunable hyperbolic metamaterial, Nat. Nanotechnol. 10 (2015) 682–686, https://doi.org/10.1038/nnano.2015.131.

[23] W.L. Song, P. Wang, L. Cao, A. Anderson, M.J. Meziani, A.J. Farr, Y.-P. Sun, Polymer/boron nitride nanocomposite materials for superior thermal transport performance, Angew. Chem. 51 (26) (2012) 6498–6501, https://doi.org/10.1002/anie.201201689.

[24] B.S. Singu, S. Palaniappan, K.R. Yoon, Polyaniline–nickel oxide nanocomposites for supercapacitor, J. Appl. Electrochem. 46 (2016) 1039–1047, https://doi.org/10.1007/s10800-016-0988-3.

[25] R.S. Kate, S.A. Khalate, R.J. Deokate, Overview of nanostructured metal oxides and pure nickel oxide (NiO) electrodes for supercapacitors: a review, J. Alloys Compd. 734 (2018) 89–111, https://doi.org/10.1016/j.jallcom.2017.10.262.

[26] T.P. Mokoena, H.C. Swart, D.E. Motaung, A review on recent progress of p-type nickel oxide based gas sensors: future perspectives, J. Alloys Compd. 805 (2019) 267–294, https://doi.org/10.1016/j.jallcom.2019.06.329.

[27] X. Yin, Y. Guo, H. Xie, W. Que, L.B. Kong, Nickel oxide as efficient hole transport materials for perovskite solar cells, Sol. RRL 3 (5) (2019), 1900001, https://doi.org/10.1002/solr.201900001.

[28] K. Singh, A. Thakur, A. Awasthi, A. Kumar, Structural, morphological and temperature-dependent electrical properties of BN/NiO nanocomposites, J. Mater. Sci. Mater. Electron. 31 (2020) 13158–13166, https://doi.org/10.1007/s10854-020-03867-w.

[29] K. Singh, M. Kaur, I. Chauhan, R. Meena, J. Singh, A. Thakur, A. Kumar, Tailoring of structural, morphological and optical properties of boron nitride/nickel oxide (BN_{100-x}/NiO_x) nanocomposites, J. Cluster Sci. 32 (2021) 865–873, https://doi.org/10.1007/s10876-020-01853-0.

[30] K. Singh, M. Kaur, I. Chauhan, A. Awasthi, M. Kumar, A. Thakur, A. Kumar, BN/NiO nanocomposites: structural, defect chemistry and electrical properties in hydrogen gas atmosphere, Ceram. Int. 46 (16) (2020) 26233–26237, https://doi.org/10.1016/j.ceramint.2020.07.084.

[31] A. Thakur, V. Sharma, G.S.S. Saini, N. Goyal, S.K. Tripathi, Effect of light intensity and temperature on the recombination mechanism in a-$(Ge_{20}Se_{80})_{99.5}$ $Cu_{0.5}$ thin film, J. Phys. D Appl. Phys. 38 (2005) 1959, https://doi.org/10.1088/0022-3727/38/12/016.

[32] J.Y. Park, S.M. Kim, H. Lee, L.I. Nedrygailov, Hot-electron-mediated surface chemistry: toward electronic control of catalytic activity, Acc. Chem. Res. 48 (8) (2015) 2475–2483, https://doi.org/10.1021/acs.accounts.5b00170.

[33] K. Singh, G. Kaur, M. Kaur, I. Chauhan, M. Kumar, A. Thakur, A. Kumar, Photoconductivity of gold nanoparticles loaded boron nitride/nickel oxide nanocomposites, Chem. Phys. Lett. 762 (2021), 138153, https://doi.org/10.1016/j.cplett.2020.138153.

[34] Y. Zhang, S. He, W. Guo, Y. Hu, J. Huang, J.R. Mulcahy, W.D. Wei, Surface-plasmon-driven hot electron photochemistry, Chem. Rev. 118 (6) (2018) 2927, https://doi.org/10.1021/acs.chemrev.7b00430.

[35] C.V. Hoang, K. Hayashi, Y. Ito, N. Gorai, G. Allison, X. Shi, Q. Sun, Z. Cheng, K. Ueno, K. Goda, H. Misawa, Interplay of hot electrons from localized and propagating plasmons, Nat. Commun. 8 (2017) 771, https://doi.org/10.1038/s41467-017-00815-x.

[36] S.M. Kim, S.W. Lee, S.Y. Moon, J.Y. Park, The effect of hot electrons and surface plasmons on heterogeneous catalysis, J. Phys. Condens. Matter 28 (2016), 254002, https://doi.org/10.1088/0953-8984/28/25/254002.